pH-Dependent Conformational Changes and Topology of a Herpesvirus Translocating Peptide in a Membrane-Mimetic Environment†

Elisabetta Schievano,‡ Tatiana Calisti,‡ Ileana Menegazzo,‡ Roberto Battistutta,‡,§ Evaristo Peggion,‡,§ Stefano Mammi,‡,§ Giorgio Palù,*,|| and Arianna Loregian||

Department of Chemical Sciences, University of Padova, 35131 Padova, Italy, Institute for Biomolecular Chemistry, CNR, 35131 Padova, Italy, and Department of Histology, Microbiology and Medical Biotechnologies, University of Padova, 35121 Padova, Italy

Received February 18, 2004; Revised Manuscript Received May 18, 2004

ABSTRACT: Pol peptide, an oligopeptide corresponding to the 27 C-terminal amino acids of DNA polymerase from herpes simplex virus type 1, has recently been suggested to translocate from endosomal compartments into the cytosol after being intracellularly delivered via a protein carrier. While an acidic environment was thought to be important for Pol peptide membrane translocation, the mechanism of translocation remains unclear. To investigate the influence of an acidic environment on the conformational properties of the peptide and on its propensity to interact with lipid bilayers, we characterized the structure of Pol peptide at different pH values by both circular dichroism (CD) and nuclear magnetic resonance (NMR) spectroscopy. The influence of detergent micelles, which mimic biological lipid membranes, on the peptide secondary structure was also studied. Our CD results indicate that the peptide is in a random conformation in aqueous solution at both acidic and basic pH, whereas in the presence of dodecylphosphocholine (DPC) micelles, it assumes a partial α-helical structure which is significantly pH-dependent. An NMR study confirmed that, in the presence of DPC micelles, a short C-terminal α-helix is present at pH 6.5, whereas almost two-thirds of the peptide (residues 10−26) fold into an extended amphipathic α-helix at pH 4.0. The orientation of Pol peptide relative to the DPC micelle was investigated using paramagnetic probes at both pH 4.0 and 6.5. These studies show that the peptide inserts deeply into the micelle at pH 4.0, whereas it is more exposed to the aqueous environment at pH 6.5. On the basis of these results, a model which might explain the mechanism of translocation of Pol peptide from acidic endosomes to the cytosol is discussed.

A number of natural and synthetic peptides are able to translocate across various cell membranes and are defined as translocating peptides or protein transduction domains. Examples of these peptides are sequences derived from homeodomains of certain transcription factors, i.e., the homeodomain-derived peptide denoted "penetratin", which corresponds to the third α-helix of the *Drosophila* Antennapedia factor (*1*), as well as so-called Tat-derived peptides (*2*, *3*) and peptides based on signal sequences (*4*, *5*). Purely synthetic or chimeric peptides with translocating properties have also been designed (*6*).

The mechanisms of translocation for the different translocating peptides are still mostly unknown. For instance, it is not known whether any particular secondary structure must be induced to allow translocation, involving a concomitant transient membrane destabilization. It is clear, however, that knowledge of the molecular details of the peptide−membrane interactions is of fundamental importance to understanding the translocation process.

We recently provided some evidence suggesting that a 27-mer (Pol peptide) derived from the C-terminus of the DNA polymerase of herpes simplex virus type 1 (HSV-1),[1] when intracellularly delivered as a fusion product with a protein carrier, the B subunit of *Escherichia coli* heat-labile enterotoxin (EtxB), is able to translocate from the endosomal compartment to the cytosol, and then into the nucleus (*7*) due to the presence of a functional nuclear localization signal (*8*). More recently, it has been reported that the inclusion of a 10-amino acid segment corresponding to the N-terminus of Pol peptide, adjacent to a class I epitope conjugated to EtxB, causes a marked increase in the extent of epitope presentation into the MHC-I pathway (*9*). These findings further suggest that Pol peptide, or part of it, is able to translocate across lipid membranes.

† This work was supported by Progetto di Ricerca di Ateneo (2000) and MURST EX60% to A.L.

* To whom correspondence should be addressed: Department of Histology, Microbiology and Medical Biotechnologies, University of Padova, via Gabelli 63, 35121 Padova, Italy. Phone: +39 049 8272350. Fax: +39 049 8272355. E-mail: giorgio.palu@unipd.it.

‡ Department of Chemical Sciences, University of Padova.

§ CNR.

|| Department of Histology, Microbiology and Medical Biotechnologies, University of Padova.

[1] Abbreviations: CD, circular dichroism; DMPG, 1,2-dimyristoyl-*sn*-glycero-3-phosphoglycerol; DPC, dodecylphosphocholine; DQF-COSY, double-quantum-filtered correlation spectroscopy; DSA, doxylstearic acid; EtxB, B subunit of *E. coli* heat-labile enterotoxin; HSV-1, herpes simplex virus type 1; NMR, nuclear magnetic resonance; NOE, nuclear Overhauser effect; NOESY, NOE spectroscopy; RA, remaining amplitude; rmsd, root-mean-square deviation; SA-MD, simulated annealing molecular dynamics; SDS, sodium dodecyl sulfate; TOCSY, total correlation spectroscopy.

10.1021/bi0496438 CCC: $27.50 © 2004 American Chemical Society
Published on Web 07/02/2004

We previously observed that Pol peptide progresses into the late stages of the endocytic pathway and can also reach the trans-Golgi network (*7*). We also reported that while brefeldin A, which disrupts the Golgi apparatus, does not affect the ability of Pol peptide to accumulate in the nucleus, both bafilomycin A1 and nocodazole, which affect the late endocytic pathway (*10*, *11*), inhibit Pol peptide nuclear localization (*7*). These observations suggested a role of late endosomal/lysosomal compartments, the environment of which is acidic, in peptide trafficking. However, the mechanism of translocation of Pol peptide from the lumen of endocytic organelles remains to be explained. Studies of the mechanism of internalization of diphtheria toxin have shown that a pH-dependent perturbation in its α-helical translocation domain occurs, permitting insertion into the lipid bilayer (*12*). Thus, the requirement for EtxB−Pol entry into acidic organelles might stem from the need to enter a pH environment that causes a structural change in Pol peptide, inducing the subsequent translocation across the membrane.

Pol peptide is part of a 36-amino acid peptide which has been subjected to detailed structural characterization. Circular dichroism (CD) spectroscopy and analytical centrifugation studies revealed that this 36-mer folds into a hairpin-like structure with partial α-helical character in aqueous solution (*13*). Further studies using multidimensional nuclear magnetic resonance (NMR) confirmed that the 36-residue peptide in aqueous solution contains partially ordered N- and C-terminal α-helices separated by a less ordered region (*14*). The 3 Å resolution of the molecular structure of the EtxB−Pol peptide fusion indicated that the 27-mer, when attached to the C-terminus of EtxB, is likely disordered (*15*). However, none of these studies has investigated whether Pol peptide undergoes a structural change upon acidification which could allow interaction with the lipid membrane and subsequent translocation.

To gain greater insight into mechanisms of Pol peptide translocation, we analyzed the peptide conformational behavior at different pH values by CD spectroscopy. Moreover, the conformational properties of Pol peptide when associated with dodecylphosphocholine (DPC) micelles, as a membrane-mimetic environment, were studied using both CD and NMR spectroscopy. The results show a significant interaction of Pol peptide with DPC micelles occurring at pH 4.0 with concomitant induction of α-helical structure in the C-terminal part of the peptide. Finally, the orientation of Pol peptide relative to DPC micelles was investigated at pH 4.0 and 6.5 using paramagnetic probes (16-doxylstearic acid, 5-doxylstearic acid, and $MnCl_2$). These studies show that the topological orientation of the peptide relative to the micelle surface is different at the two pH values.

MATERIALS AND METHODS

CD Spectroscopy. Synthesis of Pol peptide has been described previously (*16*). Spectra were acquired for 30−50 μM solutions of Pol peptide in water or in the presence of 3.7 mM DPC (Avanti Polar Lipids) micelles, of 10 mM sodium dodecyl sulfate (SDS, Fluka) micelles, or of small unilamellar vesicles composed of 5 mM 1,2-dimyristoyl-*sn*-glycero-3-phosphoglycerol (DMPG, Sigma) at various pH values. Peptide concentrations were determined by quantitative amino acid analysis. All spectra were recorded with a Jasco J-715 spectropolarimeter at 310 K. Quartz cells with Suprasil windows from HELLMA were used, with optical path lengths of 0.1 cm. All spectra were recorded in the 190−255 nm wavelength range, using a 2 nm bandwidth and a 4 s time constant at a scan speed of 20 nm/min. All spectra are reported in terms of mean residue molar ellipticity $[\theta]_R$ deg cm^2 dmol^{-1}. Data processing was carried out using a J-700 software package. The signal-to-noise ratio was improved by co-adding of at least four scans. To analyze the secondary structure content of the peptide, three different methods (*17*−*19*) were used. The results provided by all the methods were consistent with one another in the limits of the experimental errors.

NMR Spectroscopy. The NMR experiments were performed on a Bruker Avance DMX 600 spectrometer, and data were processed on an SGI Indy workstation (R5000), using the XWINNMR software. Data were collected on a 1.3 mM Pol peptide sample in a 50 mM sodium phosphate/water solution (9:1 H_2O:^2H_2O ratio) and in the presence of 140 mM DPC-d_{38} (Cambridge Isotope Laboratories) at 310 K. Under these conditions, DPC forms stable micelles. The NMR experiments were performed at pH 4.0 and 6.5. One-dimensional proton spectra were acquired with 16 transients and 32K data points. Chemical shifts were measured relative to tetramethylsilane, used as an internal reference. For sequence-specific assignments, DQF-COSY (*20*), CLEAN-TOCSY (*21*), and NOESY (*22*) spectra were used. The mixing time for the CLEAN-TOCSY spectra was 70 ms utilizing a spin-locking field of 10 kHz. In the NOESY spectra, the mixing period (70 ms) was varied randomly by ±10% to reduce zero quantum coherence contributions. All two-dimensional experiments were carried out with 512 t_1 increments of 2K data points and 32−240 scans in the phase-sensitive manner using the time-proportional phase incrementation method (*23*). The spectral width was 6000 Hz. Prior to Fourier transformation, the time domain data were multiplied by shifted sine-bell functions in the F_1 dimension and Gaussian functions in F_2; zero filling to 4K × 1K real points was employed to increase the digital resolution. In all experiments, suppression of the water signal was achieved with the WATERGATE sequence before acquisition (*24*). ^{1}H chemical shift assignments were obtained using the standard procedure developed by Wüthrich (*25*).

Structure Calculations. The volume of the NOESY cross-peaks was calculated and converted to distances using the isolated spin pair approximation and the cross-peak between a proton pair of known distance as a reference. The structures were computed from experimental restraints by using the hybrid distance geometry-dynamical simulated annealing method of Nilges *et al.* (*26*) with XPLOR (*27*). For each of the experimental situations, 150 structures of Pol peptide were obtained using simulated annealing molecular dynamics (SA-MD) calculations *in vacuo*. Of these calculated structures, 50 passed an acceptance test for bond, angle, and distance constraints. The criteria used for the acceptance were root-mean-square deviation (rmsd) for bonds of <0.01 Å, rmsd for angles of <1°, no distance violation of >0.5 Å, and dihedral angle violations of <5° which are typical of well-defined NMR structures. Among the accepted structures, 35 were chosen with the lowest total energy.

Spin-Probe Experiments. 5-Doxylstearic acid (5-DSA) and 16-doxylstearic acid (16-DSA) (Aldrich) were dissolved in methanol-d_3 (Cambridge Isotope Laboratories) to a concentration of 88 mM. Aliquots of these solutions were added to solutions of Pol peptide and DPC for a final concentration of 0.69 mM of either spin-probe ([peptide]/[spin-probe] = 1.9). $MnCl_2$ was dissolved in H_2O before being added to the sample for a final concentration of 0.19 mM. TOCSY experiments, with a mixing time of 70 ms, were recorded under identical conditions before and after the addition of the paramagnetic probes, and cross-peak intensities in the fingerprint region were compared. The results are reported in terms of the remaining amplitude (RA) of the cross-peaks, defined as

$$\mathrm{RA} = A(\mathrm{probe})/A(0)$$

where A(probe) is the amplitude of the cross-peak measured when the paramagnetic agent is added and $A(0)$ is the amplitude in the absence of the paramagnetic agent.

RESULTS

CD Spectroscopy of Pol Peptide at Different pH Values. Our previous studies aimed at identifying the compartments involved in the intracellular trafficking of Pol peptide suggested a potential role of the acidic environment of endosomal/lysosomal organelles in the translocation of the peptide from the endosomal lumen to the cytosol (*7*). Once in the cytosol, Pol peptide is able to concentrate into the nucleus due to the presence of a functional nuclear localization signal (*8*). The acidic environment could influence the conformation of Pol peptide and/or its interaction with the lipid membrane. Circular dichroism was utilized for a first characterization of the structural properties of Pol peptide under different conditions.

The CD spectrum of Pol peptide (AGFGAVGAGA-TAEETRRMLHRAFDTLA in single-letter code) in aqueous solution is typical of an essentially disordered structure (Figure 1A), independent of pH, peptide concentration, and temperature (data not shown). The CD spectra shown in Figure 1A indicate that the peptide associates with DPC micelles, undergoing a conformational transition from a disordered structure in aqueous solution to an α-helical state in the presence of DPC micelles, as evidenced by the characteristic minima at 208 and 222 nm. The maximum helical content is pH-dependent, and the system is essentially in a two-state equilibrium, as indicated by the presence of an isodichroic point at 203 nm (Figure 1A). At acidic pH, the peptide adopts a higher helical content than at basic pH, suggesting that the interaction of Pol peptide with micelles is favored at lower pH values. From the mean molar ellipticity at 222 nm (−14200 deg cm^2 dmol^{-1} at pH 4.0 and −11000 deg cm^2 dmol^{-1} at pH 8.0), we estimated α-helical contents of 45% at pH 4.0 and 28% at pH 8.0. A similar behavior in the peptide secondary structure was observed at pH 4.0 in the presence of SDS micelles and of DMPG vesicles (Figure 1B). At pH 7.4, the CD spectra in DPC and in DMPG are again very similar, while in SDS, a slightly more ordered conformation is present.

NMR-Derived Structure of Pol Peptide at Different pH Values in the Presence of DPC Micelles. The pH-dependent structure of Pol peptide was further characterized by two-

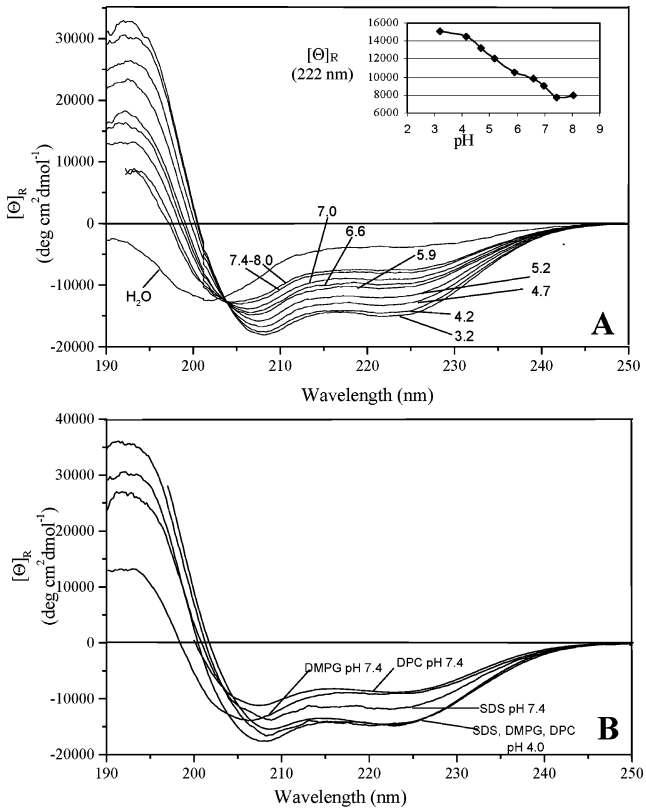

FIGURE 1: CD spectra of Pol peptide. (A) CD spectra of Pol peptide in aqueous solution and in the presence of DPC micelles (3.7 mM) at various pH values are reported. The spectra recorded in aqueous solution are independent of pH and temperature. In the inset, the residue molar ellipticity ($[\theta]_R$, deg cm^2 dmol^{-1}) at 222 nm vs pH is reported. (B) CD spectra of Pol peptide in the presence of SDS micelles (10 mM) and DMPG vesicles (5 mM) at various pH values are reported. The peptide concentration was 40 μM, and the spectra were recorded at 310 K.

dimensional NMR spectroscopy in perdeuterated DPC micelles. The micellar system of dodecylphosphocholine provides a zwitterionic lipid surface similar to that of membranes, with the advantage of a rapid reorientation in aqueous solution compared to the vesicle system, and it is therefore suitable for standard high-resolution NMR studies. A first NMR analysis was performed at pH 4.0, near the pH value of acidic lysosomal vesicular compartments. Fast exchange of the amide protons impaired their observation at neutral pH, the pH value of the cytosol environment. For this reason, the second NMR analysis was performed at pH 6.5, a point at which detection of the amide protons is still possible and the conformational transition of Pol peptide is almost complete, as indicated by the CD studies (inset of Figure 1A). The assignment of proton resonances at pH 4.0 and 6.5 is reported in Tables 1 and 2 of the Supporting Information.

The analysis of the chemical shift values of the Hα protons relative to their values in a random coil peptide (*25*) provided a first estimate of secondary structure (*28*). A local α-helical structure is identified by a negative secondary shift. The results, shown in Figure 2A, indicate the presence of a helical region extending from residue 11 to residue 25 at pH 4.0 and from residue 13 to residue 24 at pH 6.5. Chemical shift differences (>0.02 ppm) for the protons of a large number of residues between pH 6.5 and 4.0 (Figure 2B) suggest a conformational change in Pol peptide between the two pH

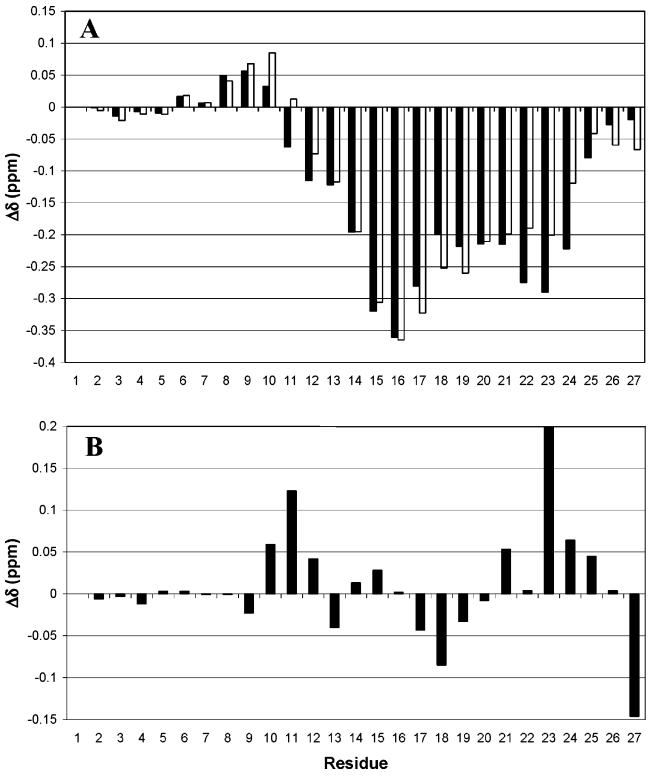

FIGURE 2: Secondary chemical shifts of H^{α} vs Pol peptide sequence. (A) Differences from the random coil chemical shifts of H^{α} for Pol peptide at pH 4.0 (black bars) and pH 6.5 (white bars) in DPC micelles at 310 K. The secondary chemical shifts are calculated as an average value over three residues. (B) Differences between the H^{α} chemical shifts at pH 6.5 and 4.0.

values. The largest changes in chemical shift were observed at both ends of the helix, indicating a possible unfolding of the extremities at pH 6.5.

Significant changes in the number and magnitude of medium-range NOEs were also observed between the two pH values. The NOE correlations are illustrated in Figure 3. At pH 4.0 (Figure 3A), a continuous pattern of $i-i+3$ and $i-i+4$ and HN(i)−HN($i+1$) NOE connectivities indicates the presence of an α-helical structure which could begin around residue 9 and extend to the C-terminal end of the peptide sequence. The absence of medium-range NOEs involving the first eight residues is an indication of random conformation. The NOE correlations at pH 6.5 are reported in Figure 3B. The lack of medium-range $i-i+3$ NOEs not only in the N-terminus but also in residues 8−13 is evident. Numerous medium-range NOEs involving C-terminal residues 24−27 are also missing which confirms the reduction of the helical segment at that pH.

The three-dimensional structures of Pol peptide at pH 4.0 and 6.5 were calculated on the basis of a total of 209 NOEs (92 intraresidue and 117 interresidue) at pH 4.0 and 177 NOEs (92 intraresidue and 85 interresidue) at pH 6.5. A superposition of the structures at pH 4.0 is shown in Figure 4A. The backbone rmsd for residues 10−26 is 0.23 ± 0.09 Å. From Figure 4A, it is clear that the first eight residues of the peptide are completely disordered, while a well-defined α-helix is present between residues 10 and 26. At pH 6.5, the α-helix is shorter, extending from residue 15 to residue 24. A superposition of the structures at pH 6.5 is shown in Figure 4B. The rmsd of the backbone atoms over residues 15−23 is 0.5 ± 0.2 Å. The average ϕ and ψ angles recovered from the calculations are reported in Tables 3 and 4 of the Supporting Information.

The marked differences between the structures of Pol peptide at pH 4.0 and 6.5 are principally localized at the extremities of the helix. The C-terminal part of the molecule is more disordered at higher pH, and the structure of residues 10−14 at pH 6.5 differs substantially from that observed at pH 4.0. Specifically, a correlation between T11 Hβ and E13 NH, observed exclusively at pH 6.5, is compatible with a transient 3_{10}-helical conformation present at this pH and identified in ∼30% of the accepted structures. To highlight the structural differences between conformations at pH 4.0 and 6.5, the ribbon diagram of the two lowest-energy structures, with the side chains included, is shown in panels C and D of Figure 4, respectively.

Paramagnetic Broadening Studies. To determine the position of Pol peptide relative to the DPC micelle at both pH 4.0 and 6.5, we used spin-probes 5-DSA and 16-DSA as well as Mn^{2+} ions ($MnCl_2$) to induce selective broadening of resonances from amino acids close to the paramagnetic probes. It has been shown that the ^{13}C and ^{1}H line broadening caused by 5-DSA is most pronounced for detergent resonances near the polar headgroup, whereas the effect of 16-DSA is largest at the apolar end of the carbon chain (*29*, *30*). At low concentrations, Mn^{2+} primarily affects resonances of water and of the protons on the surface of the micelle (*31*). EPR and NMR experiments showed that 60% of this ion is bound to the phosphate group of the micelle, while the rest of Mn^{2+} is free in the solution bulk (E. Schievano, unpublished results).

A spin-probe concentration of 0.69 mM for 5-DSA and 16-DSA and 0.19 mM for Mn^{2+} was found to be most appropriate for optimal, strong, and specific broadening effects in the spectrum of 1.3 mM Pol and 140 mM DPC samples. Under these conditions, the ratio of spin-probes to micelles is smaller than one with an assumed micelle concentration of 2.3 mM (60 DPC molecules per micelle), so interactions between spin-probe molecules can be neglected.

All three spin-labels did not change the proton chemical shifts, indicating that they have little or no effect on peptide conformation. The weak cross-peak of Ala12, even in the absence of the spin-probe, prevented an estimation of RA for this residue.

pH 4.0. The results of the experiments conducted with Mn^{2+} are shown in Figure 5A. The cross-peak intensities in the region from residue 2 to residue 20 of Pol peptide were not affected (RA > 0.8) by the addition of the salt, suggesting that the N-terminal disordered part and the first three turns of the α-helix of Pol peptide are excluded from the bulk solvent. On the contrary, cross-peak intensities of the last four residues were completely lost upon addition of Mn^{2+} (RA < 0.6), indicating an exposure to the solvent of the C-terminal part.

At pH 4.0, the addition of 5-DSA caused considerable reduction in the intensity of the HN−Hα cross-peaks for most residues (Figure 5A). Residues 2−10 were all strongly influenced by the probe, whereas a periodicity in the RA versus residue number was apparent in the C-terminal helical segment. The most affected residues (Arg16, Leu19, His20, Ala22, Phe23, Leu26, and Ala27) are localized on the

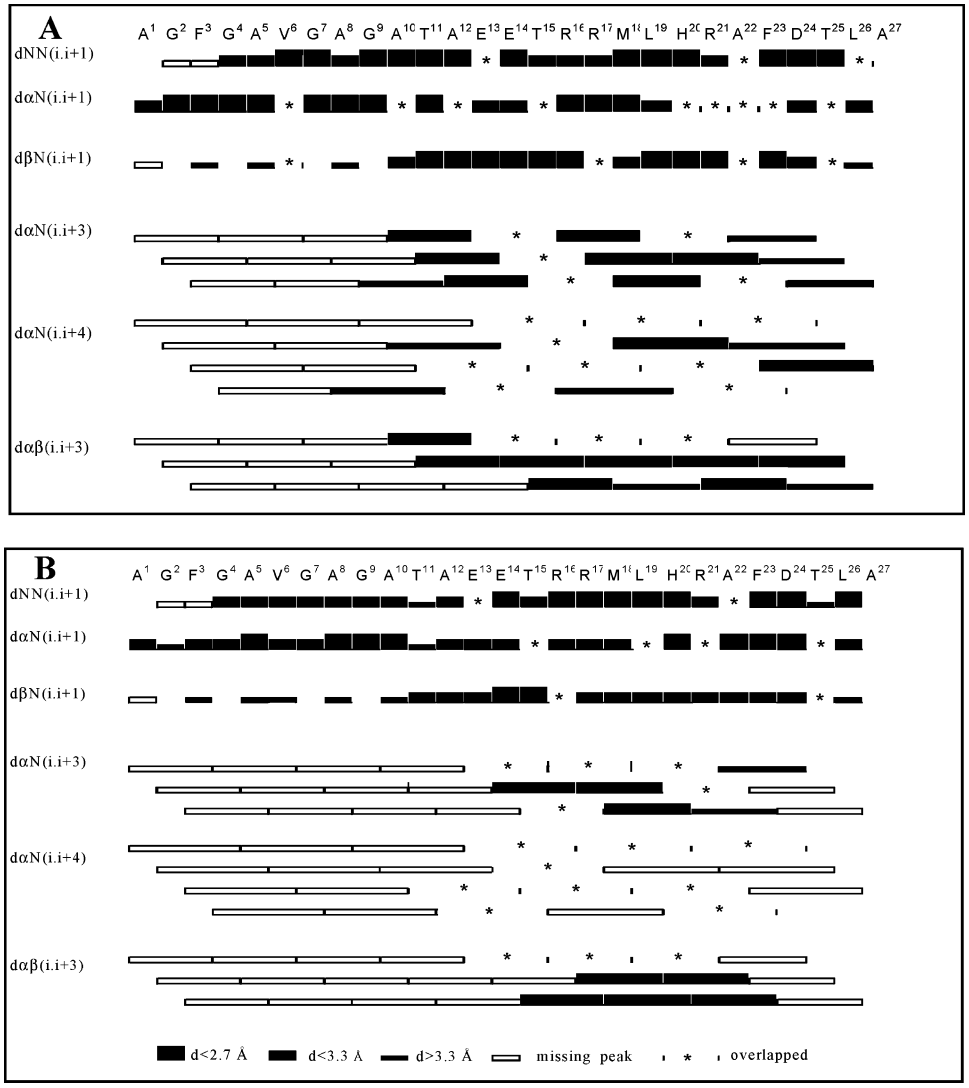

FIGURE 3: Summary of sequential and medium-range NOESY connectivities of 1.3 mM Pol peptide in 140 mM DPC at 310 K and pH 4.0 (A) and pH 6.5 (B). Peaks are grouped into three classes on the basis of their integrated volumes.

hydrophobic face of the helix, whereas the resonances of the hydrophilic residues on the opposite side of the helix are only partially reduced by 5-DSA. These results suggest that the disordered N-terminal portion of Pol peptide is positioned below the hydrophilic heads of the DPC micelles and that the helical part lies parallel to the micelle surface with the hydrophobic face toward the micelle interior.

A similar but less marked effect was observed upon addition of 16-DSA (Figure 5A). In the N-terminal part of the peptide, the same residues were affected more by 5-DSA than by 16-DSA, suggesting that the latter probe is farther from this region. This effect could be interpreted as a preference of the hydrophobic disordered segment to remain just below the surface rather than to be inserted in the core of the micelle. In the α-helical part of the molecule, also 16-DSA caused a periodic reduction of cross-peak intensities, with a less pronounced effect than in the case of 5-DSA. The fact that the cross-peaks of the resonances of the C-terminal residues were affected by both Mn^{2+} and 5-DSA may be attributed to a rapid distribution of these residues between the interior of the micelle and the water phase. In Figure 6A, the helical wheel of the segment spanning residues 10−27 summarizes the effects of both DSA spin-probes at pH 4.0.

pH 6.5. The results of the experiments conducted in the presence of Mn^{2+} (Figure 5B) were remarkably different from those obtained at pH 4.0. At pH 6.5, almost all cross-peak intensities were completely lost upon addition of this spin-probe; the magnitude of the effect rapidly increased in the first N-terminal residues and was quite pronounced for the other residues. These data suggest that the peptide is more solvent-exposed at pH 6.5 than at pH 4.0.

The effect of both DSA spin-probes at pH 6.5, reported in Figure 5B, was in general weaker than the effect at pH 4.0. The addition of 5-DSA led to a marked reduction of the cross-peak intensities in the first 10 residues of Pol peptide, as observed at pH 4.0. On the other hand, the effect of 5-DSA on residues 13 and 14 was remarkably weaker at pH 6.5 than the effect observed at pH 4.0. This result is in line with the change in structure found in this region using NOE data. In the helical part of the molecule, again, a periodicity in the RA versus residue number plot is apparent. The helical periodicity is lost for the last five residues which were not affected by 5-DSA, in agreement with the loss of ordered conformation in this region at pH 6.5 as obtained from structure calculations.

The effect of 16-DSA was weaker and more selective. In the N-terminal part, only Val6 and Gly7 exhibited a

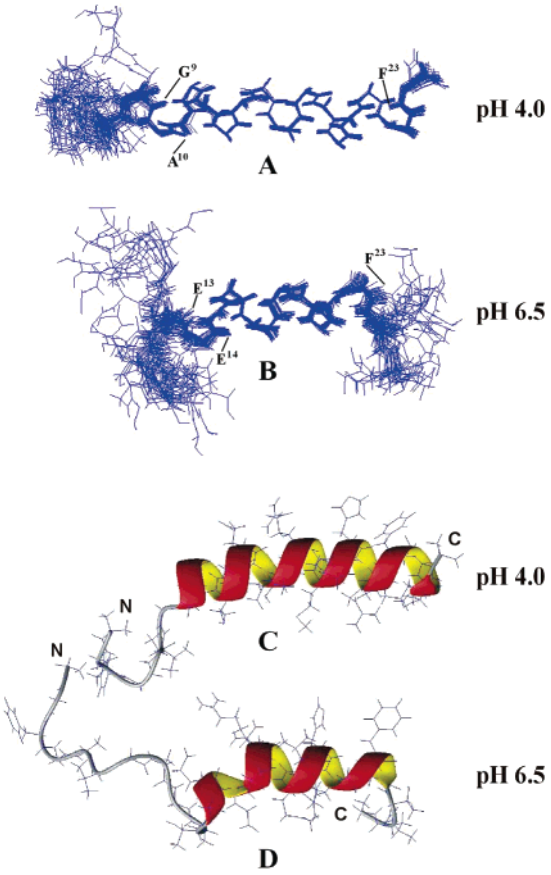

FIGURE 4: Comparison of Pol peptide structure at pH 4.0 and 6.5. Backbone representation of Pol peptide. (A) Best fit superimposition of the 35 lowest-energy structures at pH 4.0. The backbone atoms of residues 9−27 were superimposed. (B) Best fit superimposition of the 35 lowest-energy structures at pH 6.5. The backbone atoms of residues 15−23 were superimposed. (C) Backbone ribbon diagram of one of the lowest-energy structures of Pol peptide at pH 4.0. (D) Backbone ribbon diagram of one of the lowest-energy structures of Pol peptide at pH 6.5. These images were generated with MOLMOL (*47*).

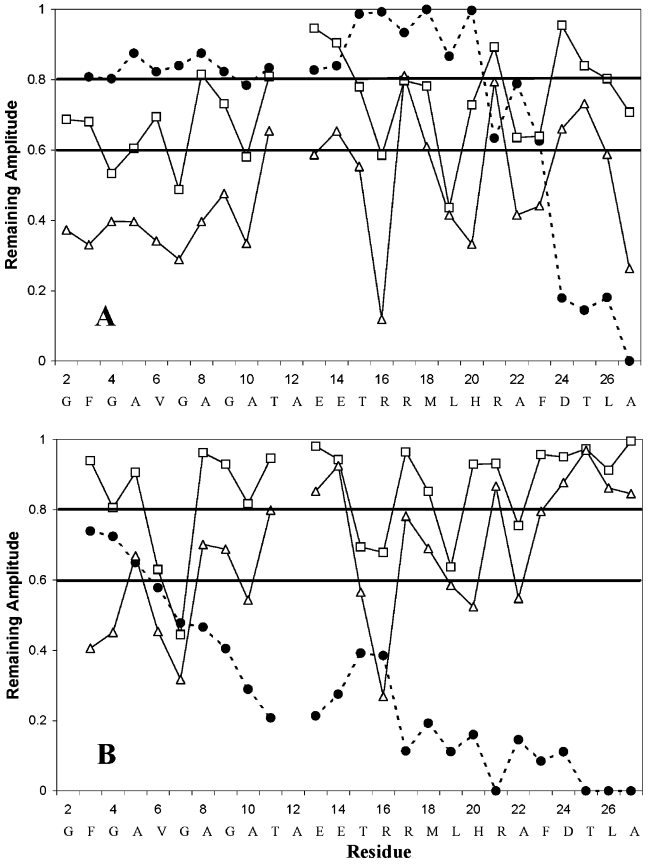

FIGURE 5: Effect of spin-probes on HN−Hα resonances of Pol peptide at pH 4.0 and 6.5. Remaining amplitude of the HN−Hα cross-peaks in the TOCSY spectra upon addition of 0.69 mM 5-DSA (△), 0.69 mM 16-DSA (■), and 0.19 mM $MnCl_2$ (●) at pH 4.0 (A) and pH 6.5 (B). Two lines at RA values of 0.8 and 0.6 delimit three ranges of the paramagnetic effect on the cross-peak intensities. When RA > 0.8, the cross-peak is considered unaffected. When RA < 0.6, the cross-peak intensity is considered completely lost.

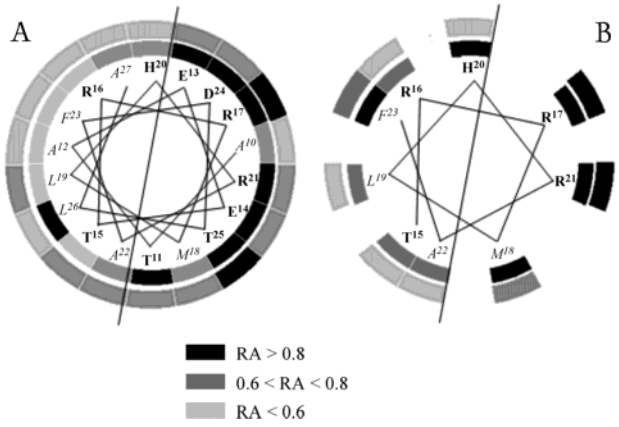

FIGURE 6: Helical wheel of the α-helical segment of Pol peptide. Helix projection along the main axis at pH 4.0 (A) and pH 6.5 (B). The hydrophobic and hydrophilic faces are divided by a black line. The apolar residues are in italics, and the polar ones are in bold. The light gray, dark gray, and black sectors in the circular crowns indicate the RA intervals caused by the effect of 5-DSA (outer sectors) and 16-DSA (inner sectors).

substantial loss of cross-peak intensity, whereas cross-peaks of residues up to Thr11 were not modified. The rest of the molecule was also hardly affected by this spin-probe, and the helical periodicity was barely present. These data indicate that, at pH 6.5, Pol peptide is farther from the core of the micelle than at pH 4.0. In Figure 6B, the helical wheel of the segment spanning residues 15−24 summarizes the effects of both 5-DSA and 16-DSA at pH 6.5.

Taken together, these observations suggest that at pH 6.5 Pol peptide is localized at the surface of the micelle with the N-terminal part immersed just below the surface, whereas the rest of the molecule is rather exposed to the bulk water. In the region spanning residues 11−14, a weaker effect of both DSA spin-probes, paralleled by a stronger effect in the presence of $MnCl_2$, indicates an increased level of exposure of these residues to the solvent at pH 6.5 than at pH 4.0.

DISCUSSION

We previously provided some evidence suggesting that a 27-residue fragment (Pol peptide) derived from the C-terminus of HSV-1 DNA polymerase possesses the ability to translocate across biological membranes (*7*). This suggestion was recently supported by another study, reporting that the inclusion of a 10-amino acid segment corresponding to the N-terminus of Pol peptide, adjacent to a class I epitope conjugated to EtxB, caused a marked increase in the extent of epitope presentation into the MHC-I pathway (*9*). Previous studies showing that drugs which neutralize the pH of acidic organelles inhibit the nuclear localization of Pol peptide

indicated that entry into an acidic compartment is essential (*7*). However, the mechanism of Pol peptide translocation from the lumen of endocytic organelles into the cytosol remains to be explained.

An explanation for the necessity of an acidic environment could be that it can cause a structural change in Pol peptide favoring subsequent translocation across lipid membranes. This already has been reported for other peptides, for example, the influenza hemagglutinin peptide (*32*, *33*) and synthetic amphipathic peptides (*34*−*36*). Pol peptide is part of a 36-amino acid segment which has been subjected to detailed structural characterization (*13*, *14*, *37*). However, none of the previous studies has investigated whether Pol peptide undergoes a conformational change upon acidification which could allow interaction with the lipid membrane and subsequent translocation.

To test this hypothesis, we characterized the structure of Pol peptide at different pH values, both in the absence and in the presence of a membrane-mimicking solvent, i.e., DPC. In fact, the DPC micelle is considered to be a simple mimic of the amphipathic environment of a phospholipid bilayer and of the bilayer−water interface (*38*). The structure of Pol peptide in aqueous solution is mostly random, independent of pH, whereas in the presence of DPC micelles, the peptide adopts a partially α-helical structure. Most interestingly, both CD and NMR studies demonstrated that there are marked differences between the structure of Pol peptide bound to DPC micelles at pH 4.0 and that at pH 6.5. In fact, a short C-terminal α-helix is present at pH 6.5, spanning residues 15−24, but the first 14 and the last three residues of the peptide are disordered. As the pH is decreased from 6.5 to 4.0, Pol peptide undergoes a conformational change which leads to the formation of a longer, well-defined amphipathic α-helix which includes almost two-thirds of the peptide (residues 10−26) and presents opposite polar and apolar faces (see also Figure 6).

The driving force for this pH-dependent conformational change is likely to be the neutralization of the carboxylate side chains of Glu13, Glu14, Asp24, and the C-terminal one. In fact, these acidic residues are positioned at the edges of the helical stretch. Specifically, the Glu residues are not included in the α-helix at pH 6.5, while at pH 4.0, they are and the helix extends three more residues toward the N-terminus. The ϕ and ψ angles of Asp24 are consistent with an α-helix at both pH values, but the helix is interrupted at residue 24 at pH 6.5, and continues to the C-terminus at pH 4.0. Charge neutralization of the carboxyl groups possibly removes unfavorable interactions between the two consecutive Glu side chains which in turn allows an N-terminal extension of the helix up to Ala10, in agreement with the tendency of this sequence to adopt an α-helical structure (*39*). In some of the structures resulting from the MD simulations at pH 6.5, a type III β-turn was detected around the Glu residues. A close inspection of the sequence reveals the possibility of side chain−side chain interaction between Glu13 and Arg16 and between Glu14 and Arg17. These $i-i+3$ interactions stabilize 3_{10}-helices and destabilize α-helices (*40*, *41*). This observation is consistent with the fact that only when these interactions are prevented through the protonation of the carboxylic functions is the presence of an α-helix observed. As far as the C-terminal region is concerned, similar arguments involving possible repulsion of the two carboxylic moieties in the main chain and in the Asp24 side chain might be proposed. These two groups would be brought into proximity by the formation of an α-helix, and this is prevented by unfavorable electrostatic interactions. In both cases, it is also possible that stronger solvation of the charged carboxyl groups by the bulk water prevails over the formation of a regular structure embedded in the membrane-mimetic milieu. The higher pH could play a role in assisting the separation of the peptide from the membrane surface by favoring interactions with the solvent. Evidence for this can be found in the studies performed in the presence of paramagnetic probes (*vide infra*).

Different effects of amphipathic peptides have been reported on model membrane systems and on cell membranes. On one hand, insertion of amphipathic peptides perpendicular to the membrane plane has been observed, leading to the formation of pores or ion channels (*42*, *43*). On the other hand, it has been shown that the adsorption of amphipathic peptides parallel to the membrane surface can occur with shallow penetration of the hydrophobic face into the apolar core of the bilayer followed by the formation of peptidic bundles or monolayers (*44*). Accumulation can result in the translocation of the amphipathic peptide by lipid reorganization that causes transient holes (*45*), hexagonal H_{II} phases, or reverse micelle formation (*46*). These three effects could occur concomitantly or independently, but all these different processes suggest an accumulation of the peptide at the surface of the membrane as a first step. Therefore, it is possible that the folding of Pol peptide in a partial amphipathic α-helical structure with opposite polar and nonpolar faces allows interaction with lipid membranes, favoring its translocation.

To address this hypothesis, the topology of Pol peptide relative to the surface and the interior of the DPC micelle at both pH 4.0 and 6.5 was investigated using paramagnetic probes, such as Mn^{2+}, 5-DSA, and 16-DSA. These paramagnetic probes are expected to cause broadening of the resonances from residues outside the micelle (Mn^{2+}), inside the micelle but close to its surface (5-DSA), and deeply buried in the micelle (16-DSA). The dimensions of the micelles are comparable with those of the peptide, which may result in a peptide−micelle interaction different from that of the peptide with the membrane. Nevertheless, the information about positioning could be useful in understanding the mechanism of translocation of Pol peptide across membranes. In fact, the micelle has the advantage of providing a simplified system for dissecting processes occurring at the lipid−water interface. Figure 7 shows a schematic picture of the disposition of Pol peptide, relative to the DPC micelle surface, at pH 4.0 and 6.5, and summarizes the information from paramagnetic broadening experiments. The global picture that emerges from these experiments is that at pH 4.0, the N-terminal disordered part and the first three turns of the α-helix of Pol peptide are deeply buried in the micelle, while the last turn of the C-terminal amphipathic α-helix lies parallel to the micelle surface with the hydrophobic face toward the interior. At pH 6.5, Pol peptide is localized at the surface of the micelle, with the N-terminal part immersed just below the surface and the rest of the molecule rather exposed to the bulk water.

From these observations, the following model explaining the mechanism of Pol peptide membrane translocation can

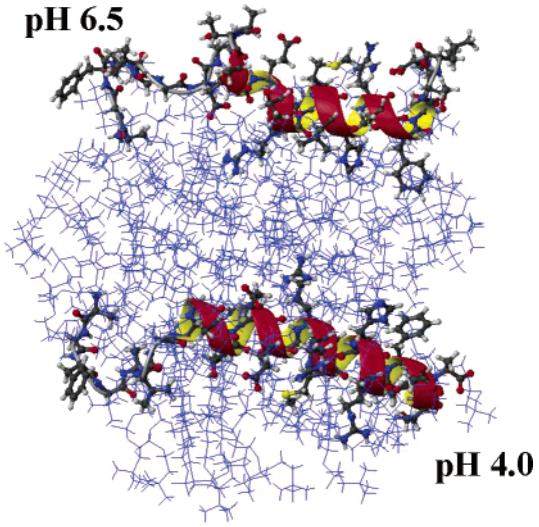

FIGURE 7: Topological disposition of Pol peptide with respect to the DPC micelle at pH 4.0 and 6.5. Cartoon of a section of a DPC micelle (blue) in which representative NMR structures of Pol peptide were positioned according to experimental spin-probes results at pH 4.0 (bottom) and pH 6.5 (top). The deeper penetration of Pol peptide at pH 4.0 can be appreciated. This image was generated with MOLMOL (*47*).

be inferred. Following endocytosis of the EtxB−Pol fusion protein, Pol peptide passes through different locales of the endocytic pathway, initially bound to EtxB and later as a separated component because of proteolytic cleavage from the fusion protein (*7*). Entry into acidic late endosomal or lysosomal organelles might cause charge neutralization by protonation of the few acidic residues in Pol peptide, i.e., Glu13, Glu14, and Asp24, favoring the interaction of the peptide with the endosomal membrane and therefore the induction of an amphipathic helical structure which favors insertion into the lipid bilayer. The contact with a nonacidic environment on the other side, namely, the cytosolic compartment, could then cause a significant loss of helical structure, which decreases the propensity of Pol peptide to interact with the lipid bilayer, resulting in the release of the peptide into the cytosol.

The studies presented here could contribute to a better understanding of the translocation process both of Pol peptide and, more in general, of other translocating peptides, and could also open up new opportunities for further exploiting Pol peptide for the intracellular delivery of immunodominant epitopes and other heterologous molecules.

ACKNOWLEDGMENT

We thank Howard S. Marsden for kindly providing part of Pol peptide used in this study and Alessandro Moretto for the rest of Pol peptide. We also thank Silvia Boso and Alessandro Case for assistance with CD spectroscopy. We gratefully acknowledge Giuseppe Zanotti and Arianna Calistri for critical reading of the manuscript.

SUPPORTING INFORMATION AVAILABLE

Tables with chemical shift assignments of the proton resonances as well as tables containing average torsion angles of the structures, recovered from the lowest-energy conformation, of the peptide in DPC micelles, at the two pH values. This material is available free of charge via the Internet at http://pubs.acs.org.

REFERENCES

1. Derossi, D., Joliot, A. H., Chassaing, G., and Prochiantz, A. A. (1994) The third helix of the Antennapedia homeodomain translocates through biological membranes, *J. Biol. Chem. 269*, 10444−10450.
2. Frankel, A. D., and Pabo, C. O. (1988) Cellular uptake of the Tat protein from human immunodeficiency virus, *Cell 55*, 1189−1193.
3. Vives, E., Brodin, P., and Lebleu, B. (1997) A truncated HIV-1 Tat protein basic domain rapidly translocates through the plasma membrane and accumulates in the cell nucleus, *J. Biol. Chem. 272*, 16010−16017.
4. Liu, K. Y., Timmons, S., Lin, Y. Z., and Hawiger, J. (1996) Identification of a functionally important sequence in the cytoplasmic tail of integrin β_3 by using cell-permeable peptide analogs, *Proc. Natl. Acad. Sci. U.S.A. 93*, 11819−11824.
5. Zhang, L., Torgerson, T. R., Liu, X., Timmons, S., Colosia, A. D., Hawiger, J., and Tam, J. P. (1998) Preparation of functionally active cell-permeable peptides by single-step ligation of two peptide modules, *Proc. Natl. Acad. Sci. U.S.A. 95*, 9184−9189.
6. Pooga, M., Hallbrink, M., Zorko, M., and Langel, U. (1998) Cell penetration by transportan, *FASEB J. 12*, 67−77.
7. Loregian, A., Papini, E., Satin, B., Marsden, H. S., Hirst, T. R., and Palù, G. (1999) Intranuclear delivery of an antiviral peptide mediated by the B subunit of *Escherichia coli* heat-labile enterotoxin, *Proc. Natl. Acad. Sci. U.S.A. 96*, 5221−5226.
8. Loregian, A., Piaia, E., Cancellotti, E., Papini, E., Marsden, H. S., and Palù, G. (2000) The catalytic subunit of herpes simplex virus type 1 DNA polymerase contains a nuclear localization signal in the UL42-binding region, *Virology 273*, 139−148.
9. De Haan, L., Hearn, A. R., Rivett, A. J., and Hirst, T. R. (2002) Enhanced delivery of exogenous peptide into the class I processing and presentation pathway, *Infect. Immun. 70*, 3249−3258.
10. Bowman, E. J., Siebers, A., and Altendorf, K. H. (1988) Bafilomycins: a class of inhibitors of membrane ATPases from microorganisms, animal cells and plant cells, *Proc. Natl. Acad. Sci. U.S.A. 85*, 7972−7976.
11. De Brabander, M., Nuydens, R., Geerts, H., and Hopkins, C. R. (1988) Dynamic behaviour of the transferrin receptor followed in living epidermoid carcinoma (A431) cells with nanovid microscopy, *Cell Motil. Cytoskeleton 9*, 30−47.
12. Kaul, P., Silverman, J., Shen, W. H., Blanke, S. R., Huynh, P. D., Finkelstein, A., and Collier, R. J. (1996) Roles of Glu 349 and Asp 352 in membrane insertion and translocation by diphtheria toxin, *Protein Sci. 5*, 687−692.
13. Digard, P., Williams, K. P., Henley, P., Brooks, I. S., Dahl, C. E., and Coen, D. M. (1995) Specific inhibition of herpes simplex virus DNA polymerase by helical peptides corresponding to the subunit interface, *Proc. Natl. Acad. Sci. U.S.A. 92*, 1456−1460.
14. Bridges, K. G., Hua, Q., Brigham-Burke, M. R., Martin, J. D., Hensley, P., Dahl, C. E., Digard, P., Weiss, M. A., and Coen, D. M. (2000) Secondary structure and structure−activity relationships of peptides corresponding to the subunit interface of herpes simplex virus DNA polymerase, *J. Biol. Chem. 275*, 472−478.
15. Matkovic-Calogovic, D., Loregian, A., D'Acunto, M. R., Battistutta, R., Tossi, A., Palù, G., and Zanotti, G. (1999) Crystal structure of the B subunit of *Escherichia coli* heat-labile enterotoxin carrying peptides with anti-herpes simplex virus type 1 activity, *J. Biol. Chem. 274*, 8764−8769.
16. Marsden, H. S., Murphy, M., McVey, G. L., MacEachran, K. A., Owsianka, A. M., and Stow, N. D. (1994) Role of the carboxy terminus of herpes simplex virus type 1 DNA polymerase in its interaction with UL42, *J. Gen. Virol. 75*, 3127−3135.
17. Greenfield, N., and Fasman, G. D. (1969) Computed circular dichroism spectra for the evaluation of protein conformation, *Biochemistry 8*, 4108−4116.
18. Chen, Y. H., Yang, J. T., and Chaun, K. H. (1974) Determination of the helix and beta form of proteins in aqueous solution by circular dichroism, *Biochemistry 13*, 3350−3359.
19. Bohm, G., Muhr, R., and Jaenicke, R. (1992) Quantitative analysis of protein far UV circular dichroism spectra by neural networks, *Protein Eng. 5*, 191−195.
20. Derome, A. E., and Williamson, M. P. (1990) Rapid-pulsing artifacts in double-quantum-filtered COSY, *J. Magn. Reson. 88*, 177−185.

21. Bax, A., and Davis, D. G. (1985) Mlev-17-based two-dimensional homonuclear magnetization transfer spectroscopy, *J. Magn. Reson. 65*, 355−360.
22. Jeener, J., Meier, B. H., Bachmann, P., and Ernst, R. R. (1979**)** Investigation of exchange process by two-dimensional NMR spectroscopy, *J. Chem. Phys. 71*, 4546−4553.
23. Marion, D., and Wuthrich, K. (1983) Application of phase sensitive two-dimensional correlated spectroscopy (COSY) for measurements of ^{1}H-^{1}H spin−spin coupling constants in proteins, *Biochem. Biophys. Res. Commun. 113*, 967−974.
24. Piotto, M., Saudek, V., and Skelnar, V. J. (1992) Gradient-tailored excitation for single quantum NMR spectroscopy of aqueous solution, *J. Biomol. NMR 2*, 661−665.
25. Wüthrich, K. (1986) *NMR of Proteins and Nucleic Acids*, John Wiley and Sons, New York.
26. Nilges, M., Clore, G. M., and Gronenborn, A. M. (1988) Determination of three-dimensional structures of proteins from interproton distance data by hybrid distance geometry-dynamical simulated annealing calculations, *FEBS Lett. 229*, 317−324.
27. Brunger, A. T. (1992) *X-PLOR version 3.0, A system for X-ray crystallography and NMR*, Yale University Press, New Haven, CT.
28. Pastore, A., and Saudek, U. (1990) The relation between chemical shift and secondary structure of proteins, *J. Magn. Reson. 90*, 165−176.
29. Van Den Hooven, H. W., Spronk, C. A., Van De Kamp, M., Konings, R. N., Hilbers, C. W., and Van De Ven, F. J. (1996) Surface location and orientation of the lantibiotic nisin bound to membrane-mimicking micelles of dodecylphosphocholine and of sodium dodecylsulphate, *Eur. J. Biochem. 235*, 394−403.
30. Brown, L. R., Bösch, C., and Wüthrich, K. (1981) Location and orientation relative to the micelle surface for glucagon in mixed micelles with dodecylphosphocholine, *Biochim. Biophys. Acta 642*, 296−312.
31. Lindberg, M., and Gräslund, A. (2001) The position of the cell penetrating peptide penetratin in SDS micelles determined by NMR, *FEBS Lett. 497*, 39−44.
32. Han, X., and Tamm, L. K. (2000) pH-dependent self-association of influenza hemagglutinin fusion peptides in lipid bilayers, *J. Mol. Biol. 304*, 953−965.
33. Han, X., Bushweller, J. H., Cafiso, D. S., and Tamm, L. K. (2001) Membrane structure and fusion-triggering conformational change of the fusion domain from influenza hemagglutinin, *Nat. Struct. Biol. 8*, 715−720.
34. Parente, R. A., Nir, S., and Szoka, F. C., Jr. (1988) pH-dependent fusion of phosphatidylcholine small vesicles. Induction by a synthetic amphipathic peptide, *J. Biol. Chem. 263*, 4724−4730.
35. Parente, R. A., Nadasdi, L., Subbarao, N. K., and Szoka, F. C., Jr. (1990) Association of a pH-sensitive peptide with membrane vesicles: role of amino acid sequence, *Biochemistry 29*, 8713−8719.
36. Parente, R. A., Nir, S., and Szoka, F. C., Jr. (1990) Mechanism of leakage of phospholipid vesicle contents induced by the peptide GALA, *Biochemistry 29*, 8720−8728.
37. Zuccola, H. J., Filman, D. J., Coen, D. M., and Hogle, J. M. (2000) The crystal structure of an unusual processivity factor, herpes simplex virus UL42, bound to the C terminus of its cognate polymerase, *Mol. Cell 5*, 267−278.
38. Damberg, P., Jarvet, J., and Gräslund, A. (2001) Micellar systems as solvents in peptide and protein structure determination, *Methods Enzymol. 339*, 271−285.
39. Chou, P. Y., and Fasman, G. D. (1974) Prediction of protein conformation, *Biochemistry 13*, 222−245.
40. Schievano, E., Bisello, A., Chorev, M., Bisol, A., Mammi, S., and Peggion, E. (2001) Aib-rich peptides containing lactam-bridged side chains as models of the 3_{10}-helix, *J. Am. Chem. Soc. 123*, 2743−2751.
41. Houston, M. E., Gannon, C. L., Kay, C. M., and Hodges, R. S. (1995) Lactam bridge stabilization of α-helical peptides: ring size, orientation and positional effects, *J. Pept. Sci. 1*, 274−282.
42. Matsuzaki, K., Murase, O., Takuda, H., Funakoshi, S., Fujii, N., and Miyajima, K. (1994) Orientational and aggregational states of magainin 2 in phospholipid bilayers, *Biochemistry 33*, 3342−3349.
43. Urry, D. W., Goodall, M. C., Glickson, J. D., and Mayers, D. F. (1971) The gramicidin A transmembrane channel: characteristics of head to head dimerized π(L,D) helices, *Proc. Natl. Acad. Sci. U.S.A. 68*, 1907−1911.
44. Gazit, E., Boman, A., Boman, H. G., and Shai, Y. (1995) Interaction of the mammalian antibacterial cecropin P1 with phospholipid vesicles, *Biochemistry 34*, 11479−11488.
45. Matsuzaki, K., Murase, O., Fujii, N., and Miyajima, K. (1995) Kinetics of pore formation by an antimicrobial peptide, magainin 2, in phospholipid bilayers, *Biochemistry 34*, 6521−6526.
46. Rietveld, A., Jordi, W., and De Kruijff, B. (1986) Studies on the lipid dependency and mechanism of the translocation of the mitochondrial precursor protein apocytochrome *c* across model membrane, *J. Biol. Chem. 261*, 3846−3856.
47. Koradi, R., Billeter, M., and Wüthrich, K. (1996) MOLMOL: a program for display and analysis of macromolecular structures, *J. Mol. Graphics 14*, 51−55.

BI0496438